Received: 31 January 2021 | Revised: 14 June 2021 | Accepted: 17 June 2021

DOI: 10.1002/cjce.24253

SPECIAL ISSUE ARTICLE

THE CANADIAN JOURNAL OF CHEMICAL ENGINEERING

Canadian Society for Chemical Engineering | For Our Future
Société canadienne de génie chimique | Pour notre avenir

Computational fluid dynamic characterization of vertical-wheel bioreactors used for effective scale-up of human induced pluripotent stem cell aggregate culture

Tiffany Dang[1,2,3]† | Breanna S. Borys[1,2,3,4]† | Shivek Kanwar[1,5] | James Colter[1,2,3] | Hannah Worden[4] | Abigail Blatchford[4] | Matthew S. Croughan[6] | Tareq Hossan[7] | Derrick E. Rancourt[7] | Brian Lee[4] | Michael S. Kallos[1,2,3] | Sunghoon Jung[4]

[1]Pharmaceutical Production Research Facility, Schulich School of Engineering, University of Calgary, Calgary, Alberta, Canada

[2]Biomedical Engineering Graduate Program, University of Calgary, Calgary, Alberta, Canada

[3]Department of Chemical and Petroleum Engineering, Schulich School of Engineering, University of Calgary, Calgary, Alberta, Canada

[4]PBS Biotech Inc., Camarillo, California, USA

[5]Department of Mechanical and Manufacturing Engineering, Schulich School of Engineering, University of Calgary, Calgary, Alberta, Canada

[6]Matt Croughan Ph.D. Consulting Services, Reno, Nevada, USA

[7]Department of Biochemistry and Molecular Biology, Cumming School of Medicine, University of Calgary, Calgary, Alberta, Canada

Correspondence
Sunghoon Jung, PBS Biotech Inc., 4721 Calle Carga, Camarillo, CA 93012, USA.
Email: sjung@pbsbiotech.com

Abstract

Bioreactor-based processes are the method of choice for efficient expansion of cells in a controlled setting. However, induced pluripotent stem cells (iPSCs) have proven to be extremely sensitive to the bioreactor hydrodynamic environment, making the use of suspension bioreactors to produce quality-assured cells at clinical and commercial scales very challenging. The PBS vertical-wheel (VW) bioreactor combines radial and axial flow components to produce uniform hydrodynamic force distributions, making it a promising platform to overcome the scale-up challenges associated with iPSCs. In this study, hydrodynamic characterization through computational fluid dynamics modelling of VW bioreactors was performed. Analysis of these models proved that important volume average hydrodynamic variables could be maintained throughout scale-up from the 0.1 L to the 15 L VW bioreactor scale. Each bioreactor scale (0.1, 0.5, 3, and 15 L) was modelled at a variety of agitation rates, leading to the generation of scale-up correlation equations. These equations allow operators to define a working range of hydrodynamic variables at one scale and calculate the corresponding agitation rates at other modelled scales. A suggested operating range of agitation rates was determined for the successful culture of iPSCs in the VW bioreactor at each scale, corresponding to constant volume average energy dissipation rate. Agitation rates from the 0.1 and 0.5 L VW bioreactor scale were experimentally tested to biologically validate the suggested range. High cell-fold expansion, healthy aggregate morphology, growth, and uniformity were demonstrated for all conditions tested within the suggested working range.

KEYWORDS

computational fluid dynamics modelling, induced pluripotent stem cells, vertical-wheel bioreactor

† Co-first author.

1 | INTRODUCTION

Innovations in engineering and bioprocess development have accelerated the transition of induced pluripotent stem cell (iPSC) cultivation and use from the bench-top to large-scale clinical manufacturing.[1,2] Owing to their potency, proliferation capabilities, and ability to overcome the challenges associated with traditional sources of pluripotent stem cells (PSCs), iPSCs have generated significant interest in the field of regenerative medicine for more than a decade.[3] However, traditional bench scale methods to expand iPSCs, including petri dishes and T-flasks, are insufficient to achieve clinically relevant numbers. For iPSC treatments, cell dosages will range from 10^9–10^{12} cells per patient depending on the therapeutic target.[4] To achieve the required number of cells in an effective and scalable manner, bioreactors will need to be used. The platform has been frequently used in the biotechnology industry with advantages including reduced operating costs, reduced risks of contamination, and improved process control and monitoring.

However, a consequence of transitioning to a bioreactor-based platform is the introduction of hydrodynamic forces. It has been previously shown that the presence of hydrodynamic forces significantly impacts biological properties including cell growth, viability, pluripotency, and differentiation.[5,6] For instance, in the absence of leukaemia inhibitory factor, fluid shear stress can maintain the pluripotency of mouse PSCs.[7,8] For PSCs, which are commonly cultured as aggregates in bioreactor-based systems, hydrodynamic forces, along with other factors, influence the aggregate size through shear from the local environment and interactions of the aggregates with turbulent eddies. Aggregate size is an important parameter. Similar to microcarrier cultures, large aggregates may be damaged by small, intense eddies, which detach the outermost cells. This may occur when the eddy length is less than one-half to two-thirds of the aggregate diameter.[9] Additionally, cells within aggregates are subjected to mass transfer limitations which result in cell necrosis in the centre when the aggregate diameter is greater than 400 μm.[5,7,10] This in turn impacts both cell quality and yield.

Due to the complexities of hydrodynamic forces, it is not possible to keep all parameters constant when scaling up bioprocesses or bioreactor geometries. Scale-up equations have been generated to help choose agitation rates for bioreactors based on the optimized conditions discovered at the laboratory scale.[11] However, common hydrodynamic scale-up parameters for mammalian cell culture to predict agitation rates often rely on the maximum hydrodynamic values, such as maximum shear stress and impeller tip speed. These maximum values are not found in most of the fluid volume of the bioreactors. Only a small portion of the culture is exposed to these extreme forces at any given time, possibly decreasing the correlation between the calculated optimal agitation rate and actual optimal rate, and between these parameters and the biological behaviour of the system.

Another approach is to scale up via constant average values, such as constant average energy dissipation rate per mass (power/mass). Traditionally, this has been done through maintenance of geometric similarity upon scale up and the use of correlations between Power number and Reynolds number, measured experimentally for any given geometry. This approach is explained by Nienow along with many other bioreactor considerations for animal cell culture.[12] It has the disadvantage that one must either stick to standard, previously characterized geometries, or build all proposed novel geometries for experimental characterization. Furthermore, if the distribution of energy dissipation changes substantially upon scale up or upon small changes in geometry, a local maximum sufficient to cause damage may occur, even if average values are kept constant. Ideally, design and scale up can be done computationally, to readily consider a variety of design options and also scale up at a constant average values, but with a double check on distributions, to make sure no local maxima are hit that may lead to problems.

We have previously demonstrated that maintaining constant volume average (VA) parameters during the scale up process, such as the VA energy dissipation rate (EDR) and VA shear stress, allowed us to better maintain predictable cell growth.[13] Another limitation using scale-up equations for PSC culture is that PSC aggregate size is not solely a result of agitation rate. It is also influenced by bioreactor geometry, cell density, medium viscosity, and cell–cell adhesion strength. Traditional hydrodynamic scale-up equations are unable to account for those underlying factors.[14] Computational fluid dynamics (CFD) modelling enables the implementation of accurate and precise models across scales by generating geometry-specific scale-up equations and calculating VA hydrodynamic values.[13,15,16]

CFD models offer a cost-effective method of understanding the hydrodynamics of bioreactors in silico, reducing the number of biological experiments required to develop a scale-up process. It also enables characterization of bioreactors at any scale, giving detailed three-dimensional (3D) data as well as VA values for parameters such as velocity, shear, and EDR. Bioreactor geometries at all feasible scales can be modelled at desired agitation rates, and trendlines can be applied to generate scale-up equations. Therefore, the use of CFD modelling facilitates a more efficient transition from laboratory-scale to commercial-scale bioreactors.

In the current study, we used CFD modelling for hydrodynamic characterization of the PBS vertical-wheel (VW) bioreactors at multiple scales. We have previously demonstrated that the 0.1-L VW bioreactor combines both radial and axial flow components. This geometry produces more uniform energy dissipation distributions and lower shear stress environments.[17,18] To expand upon our previous work, we modelled additional scales of the VW bioreactor including 0.5, 3, and 15 L at various agitations as shown in Figure 1. Scale-up equations were developed from the models and used to determine a suitable operating range to culture human iPSCs (hiPSCs) where the VA EDR was maintained. By performing experiments culturing hiPSCs at the agitation rates predicted by our models, we demonstrated consistent aggregate formation at the 0.1 and 0.5 L scale using these generated equations. Using CFD modelling and subsequent biological testing, this study provides evidence that important VA hydrodynamic variables such as EDR can be maintained throughout scale-up for multiple scales and a suitable operating range can be determined.

2 | MATERIALS AND METHODS

2.1 | Computational fluid dynamics models

2.1.1 | Model set up

For this study, CFD models were completed for the 0.1, 0.5, 3, and 15 L VW bioreactors. Virtual geometry

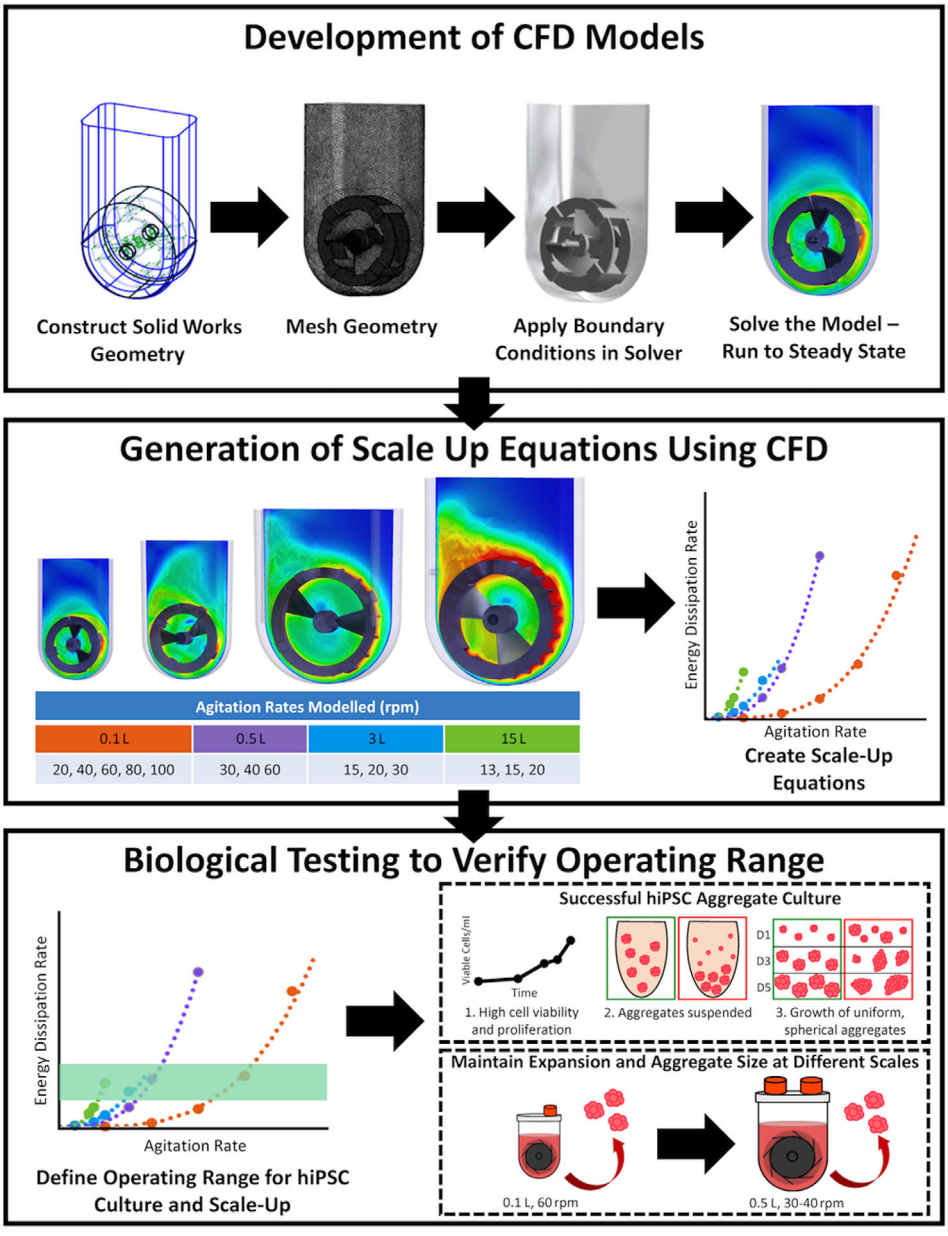

FIGURE 1 Process diagram outlining the steps taken for construction of computational fluid dynamic models of the VW bioreactors. Each VW bioreactor model was run at various agitation rates and data was post-processed to generate hydrodynamic scale-up equations. From the analyzed data, a suggested operating range was defined and biologically validated to ensure the successful culture of hiPSC aggregates that maintained expansion rates and aggregate sizes at different bioreactor scales

models were built using the computer-aided design (CAD) software SolidWorks 2020. Each virtual geometry model consisted of a rotating domain geometry and vessel domain geometry which represented the working volume of the fluid. The resulting virtual geometry model was imported into the meshing software ANSYS ICEM CFD 2019 Revision 2 where the bioreactor geometry was discretized using tetrahedral elements. The generated mesh model consisted of 400 000 elements with side lengths ranging from 0.001 525–0.007 25 m.

2.1.2 | Solving the models

To solve the models, the CFD simulating software ANSYS Fluent 2019 Revision 2 was used. A pressure-based, transient solver was adapted for use to solve models in a 3D configuration. Boundary conditions were prescribed at different surfaces. Wall boundary conditions were applied to the vessel wall and impeller, where there are no normal or tangential velocities to the vessel wall. The surface of the liquid was modelled using a zero shear and free surface boundary condition. To simulate the impeller rotation, a moving reference frame with a liquid–solid interface boundary condition was used between the rotating and stationary domains.

A realizable k-epsilon Navier Stokes model was used. The k-epsilon model is a popular turbulent model used to simulate the hydrodynamic environment in suspension bioreactors.[15,19] It utilizes Equations (1) and (2) to represent the conservation of mass and momentum:

$$\frac{\partial \rho}{\partial t} + \nabla \cdot (\rho u) = 0 \tag{1}$$

$$\frac{\partial \rho u}{\partial t} + \nabla (\rho u \otimes u) = -\nabla P + \mu \nabla^2 u + \rho g \tag{2}$$

where ρ is the density, u is the cartesian velocity vector, t is time, P is pressure, μ is viscosity, and g is the gravity vector. Water at 37°C with a density of 1006 kg/m^3 and dynamic viscosity of 8.5×10^{-4} kg/(m · s) was used to simulate the fluid inside the reactor.

All equations were discretized using a first-order upwind scheme. Figure 1 outlines the tested agitation rates for all model scales. CFD data and case files were uploaded to the Advanced Research Cluster (ARC) at the University of Calgary, utilizing part of a 40-core partition in a hybrid parallel computational configuration to solve the models. Batch and input files were written using the ARC ANSYS index and ANSYS Fluent remote reference documentation. Each model ran for a flow time of 5 s, with a time step chosen to keep the Courant-Friedrich-Lewy (CFL) number below 1. This ensured that a fluid element crossed from one side to the other for a mesh element in one time step.

2.1.3 | Post processing

Post processing was performed for all simulated models. ANSYS CFD Post 2019 Revision 2 was used to generate heat maps and distribution graphs for hydrodynamic variables including velocity and EDR. MATLAB Revision 2019a was used to plot the flow time data for velocity, EDR, shear stress, and CFL number. The flow time data was also used to generate the scale-up correlation equations used for biological testing.

2.2 | Cell culture

2.2.1 | Culture media

hiPSCs were cultured in a commercially available medium (mTeSR1, STEMCELL, 85881) and another medium formulated in-house. The home-brew (HB) medium was formulated with a modification of B8 medium,[20] consisting of DMEM (Dulbecco's Modified Eagle Medium) /Ham's F-12 50/50 with L-glutamine and 15 mM HEPES (Corning, 10-092-CM), 200 µg/ml L-ascorbic acid 2-phosphate trisodium salt (Wako, 323–44 822), 20 µg/ml recombinant human insulin (Gibco, A11382II), 20 µg/ml recombinant human transferrin (InVitria, 777TRF029), 20 ng/ml sodium selenite (Sigma, S5261), 0.1 ng/ml neuregulin (recombinant human heregulinβ-1) (Peprotech, 100–03), 20 ng/ml heat stable recombinant human bFGF (ThermoFisher, PHG0360), 0.1 ng/ml recombinant human TGF-β3 (Cell Guidance Systems, GFH109-10), and 1% non-essential amino acids (NEAA, ThermoFisher, 11 140 050). Cell culture grade water (Fisher, SH30529LS) and 1.0 M HCl (Honeywell, 35 328) were used to reconstitute the components and make stock solutions. An aliquot of 10 µM Y-27632 (STEMCELL, 72304) was added to all media and enzyme used for harvesting and passaging cells. Modifications to the published B8 medium formulation include a decreased bFGF concentration and addition of 1% NEAA. These modifications were made following a ranging concentration study (Figure S1) in the 0.1 L VW bioreactor, which showed no difference in final cell concentrations based on bFGF concentration (20–140 ng/ml was

tested) and an increase in final cell concentration with the additional of 1% NEAA.

2.2.2 | Static culture of hiPSCs

hiPSC line 4YA, derived from infant fibroblasts, was used for all experiments in this study. These cells were obtained from Dr. James Ellis' laboratory at the University of Toronto (Toronto, Ontario, Canada). The cells used were between passage numbers 46–51. All cultures were maintained at 37°C in a humidified atmosphere with 5% CO_2. The static expansion of these cells prior to bioreactor culture was performed according to methods previously described by Borys et al.[17,18] In brief, hiPSCs were grown in Matrigel-coated (Corning, 354 277) T-flasks (Thermo Scientific, 156 599) in mTeSR1 medium supplemented with 10 μM Y-27632. Media exchanges were performed daily with Y-27632-absent medium, and cells were passaged 3 days post-inoculation (at approximately 80% confluency). Cells were detached using Accutase (STEMCELL, 07920) supplemented with 10 μM Y-27632, and further diluted in fresh culture medium. The dissociated cells were collected into conical tubes, centrifuged at 500 g for 5 min, and resuspended in fresh culture medium containing 10 μM Y-27632. Duplicate samples were removed from the cell suspension and counted with a NucleoCounter NC-200 (ChemoMetec) to obtain a viable cell density.

2.2.3 | Suspension culture of hiPSCs

This study used 0.1 and 0.5 L working volume, single-use VW bioreactors (PBS Biotech). Bioreactors were batched with 95% of the working volume of culture medium and placed in the incubator (37°C and 5% CO_2) overnight. hiPSCs were inoculated as single-cells at a density of 20 000 cells/ml in culture medium supplemented with 10 μM Y-27632. Constant mixing was maintained at agitation rates of 60 rpm in the 0.1-L VW bioreactor and 18, 30, 40 and 60 rpm in the 0.5-L VW bioreactors. A 50% medium exchange (MX) was performed on day 3, day 5, and day 6 of culture with Y-27632-absent medium. For each MX, agitation was stopped and the aggregates were allowed to settle for 5 min. Each bioreactor was brought into a biosafety cabinet where media was aspirated from the top of the liquid volume in the bioreactor and added into 50-ml (0.1-L bioreactor) or 500-ml (0.5-L bioreactor) conical tubes, which were centrifuged at 500 g for 5 min to recover any cells that had not settled in the bioreactor. The supernatant was discarded, and the cell pellet was resuspended in pre-warmed fresh medium before being added back into the bioreactor.

2.2.4 | Cell counts and aggregate sizing

Samples between 1.0–5.0 ml were taken daily from the bioreactors to assess growth kinetics and aggregate morphology, using a previously described sampling and counting method by Borys et al.[18] Duplicate samples were taken, and corresponding cell counts were used to generate cell growth curves and calculate cell-fold expansion. Photomicrographs were captured using a Nikon Eclipse Ts2-Fl microscope. To determine average aggregate sizes, 1.5 ml samples were removed using a serological pipette from the bioreactors and added into 12-well plates for visualization. Images were taken using the Nikon Eclipse Ts2-F1 microscope and NIS-Elements software was used for measurements. Aggregates were defined as multicellular spheroids with a diameter greater than 50 μm. The diameter for each aggregate was determined by taking the average of the greatest length across the aggregate and the length perpendicular to the greatest length.

2.2.5 | RNA isolation, cDNA synthesis, and quantification of gene expression by quantitative real-time PCR

RNA isolation, cDNA synthesis, and gene expression analysis were performed according to the methods described by Borys et al.[18] Briefly, the hiPSCs from static and bioreactor (fed, day 6) cultures were collected. Total RNA was isolated using a PureLink RNA Mini Kit (Cat#12183018A, Thermo Fisher Scientific) according to the manufacturer protocol. Then, 1 μg of extracted RNA was used for cDNA synthesis by a ProtoScript II First Strand cDNA Synthesis Kit (Cat#E6560L, New England Biolabs). Oligo-dT primer (d[T]23VN) provided with the kit was used for reverse transcription. Next, qPCR was done using a QuantiFast SYBR Green PCR Kit (REF#20454, Qiagen GmbH) in a 10 μl reaction volume with the provided protocol. Two technical and three biological replicates of each sample were used. Relative quantification was done by normalizing with cycle threshold (CT) values of the housekeeping gene human GAPDH. Expression levels of the samples were relatively determined with the static cultured hiPSC samples. The relative quantification was performed using comparative CT (ΔΔCT) through the $2^{-\Delta\Delta CT}$ method. The pluripotency-associated genes, SOX2, KLF4, and REX1, were used for RT-qPCR. All the primer sequences were obtained from our previous study.[18]

2.2.6 | Statistical analysis

Statistical analysis was performed using GraphPad Prism (v6.0). A one-way ANOVA followed by Tukey's multiple comparison test was used for aggregate size comparison and RT-qPCR analysis. Differences were considered statistically significant at $p < 0.05$. Data are presented with mean ± standard deviation.

3 | RESULTS

3.1 | Analysis of computational fluid dynamic models of vertical-wheel bioreactors

For this study, CFD modelling was used to characterize the hydrodynamic environment of laboratory scale (0.1 and 0.5 L) to clinical and commercial scale (3 and 15 L) VW suspension bioreactors. After the models reached pseudo-steady state, post processing analysis was performed. The heat maps in Figures 2 and 3 are vertical cut planes through the centre of the reactor used to help visualize the impact of changing agitation rate on the velocity and EDR, respectively, at each bioreactor scale.

It is particularly evident in the velocity cut planes (Figure 2) that maximum hydrodynamic values occur at the outer wheel edge in the bioreactors. These red (≥0.15 m/s) areas are minimal or non-existent at the lowest modelled agitation rate at each bioreactor scale and take up a larger volume fraction as the agitation rate increases. The sweeping changes in colour from dark blue (0.0 m/s) to light blue (0.04 m/s) and green (0.08 m/s) in the upper corners of the bioreactor cut planes are indicative of the VW-impeller mixing in both a radial and axial direction. This is an essential hydrodynamic characteristic to circulate the fluid throughout the volume of the reactor. These cut planes also indicate if a condition (bioreactor scale and agitation rate) may produce too low of a fluid velocity for effective mixing. For example, the 0.1 L bioreactor scale modelled at 40 rpm (Figure 2A) does not display a change in colour (remains dark blue) in the upper portion of the vessel. This could result in a fluid dead zone where cells or cell aggregates get trapped.

The EDR cut planes in Figure 3 display less of a colour change through the bioreactor volume. The middle agitation rate modelled at each scale remains almost entirely dark blue (0.001 m^2/s^3), meaning the number of turbulent eddies should be limited throughout the bioreactor volume. This is an important hydrodynamic characteristic when working with sensitive stem cell cultures. The maximum EDR values that occur around the outer wheel are significantly higher than the VA values. For example, at the 15 L scale modelled at 13 rpm (Figure 3D), 0.01% of the reactor volume has an EDR of 1.0E-1 m^2/s^3. This maximum value is two orders of magnitude higher than the VA EDR.

It is important to note that both the velocity and EDR heat maps appear similar between the modelled agitation rates at the various scales. The colour gradient scale used for each scale bioreactor is the same to allow for this comparison. This can indicate that scale-up between the various scales should prove feasible with an ability to maintain important hydrodynamic variables when choosing the appropriate agitation rate.

3.2 | Energy dissipation rate scale-up correlations and distributions

Once each model was run at a minimum of three agitation rates, additional post-processing allowed for the generation of scale-up correlations to compare the exponential increase in VA EDR in response to an increase in agitation rate (Figure 4A). As we have demonstrated previously,[13] VA EDR does not increase in a linear fashion in response to changes in agitation rate. Other parameters, such as velocity, shear stress, or tip speed, do increase linearly with agitation rate for any given VW bioreactor (Figures S2A–C). For each VW bioreactor scale, the VA EDR at the modelled agitation rates were plotted and fitted with power equation trendlines—all resulting in R^2 values over 0.99 (Figure 4A). These correlations allow the user to optimize the hydrodynamic conditions at the smallest scale (0.1 L) and then predict the corresponding operating agitation rates at the larger scales to maintain the same VA EDR, saving resources and allowing numerous conditions to be run in parallel. We have, for example, shown that single-cell inoculation of hiPSCs in the 0.1 L VW bioreactor operated at 60 rpm will result in high cell-fold expansion and morphologically healthy and uniform aggregate growth. Using the scale-up correlation equations provided in Figure 4A, the operator can calculate that the 0.5, 3, and 15 L VW bioreactors should be operated at 30, 24, and 15 rpm, respectively, to maintain the same VA EDR through scale-up. The authors have defined a suggested working range of VA EDRs for the culture of hiPSCs inoculated as single-cells and grown as aggregates to be between 3.0E-4 and 1.5E-3 m^2/s^3. The suggested operating range was defined through analysis of the CFD generated VW cut planes and past biological testing observations.[17,18] Conditions displaying low velocity gradients, lacking sufficient mixing to suspend cell aggregates, were used to define a lower operating limit, and conditions displaying high EDR gradients, producing turbulent eddies

detrimental to cell viability, were used to define an upper operating limit. This operating range provides a range of agitation rates to work with at each VW bioreactor scale. Outside of this range, it is likely that the aggregates will become too large, clump together, and settle due to a low VA EDR, or be sheared apart with single cells unable to form strong aggregates due to a high VA EDR. Both these situations would amount to reduced proliferation, increased cell-death, and morphologically unhealthy aggregates lacking uniformity in size and shape.

From the suggested working range of agitation rates, an EDR frequency distribution graph was generated to

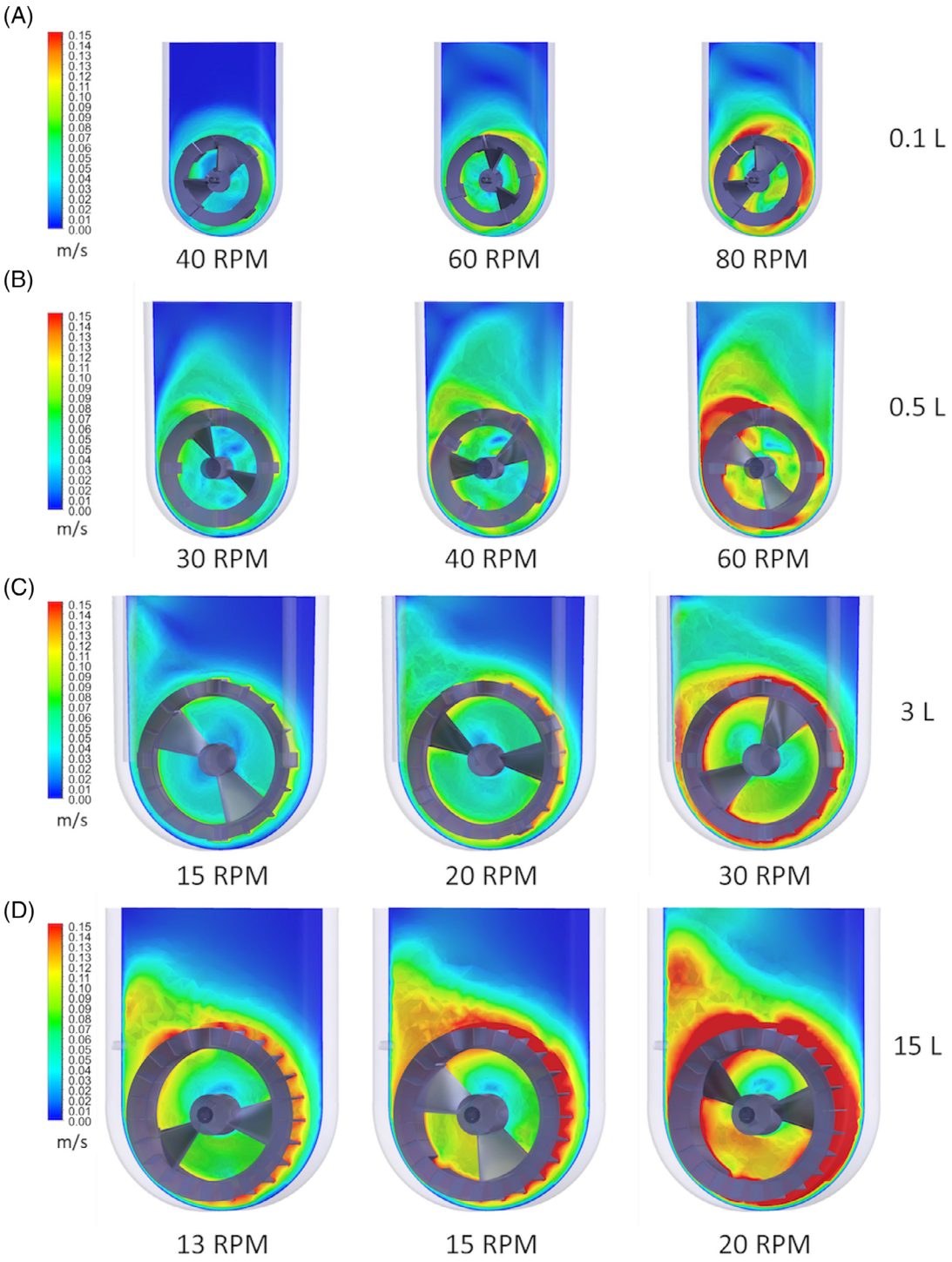

FIGURE 2 Steady-state, vertical plane heat-maps of the velocity throughout the (A) 0.1-L, (B) 0.5-L, (C) 3-L, and (D) 15-L VW bioreactor scale. These cut planes are not imaged to scale—the following wheel diameters can be used as a reference measurement: 0.1 L (43 mm), 0.5 L (72 mm), 3 L (137 mm), and 15 L (227 mm)

highlight the EDR distributions within the bioreactor volumes when operated at steady state (Figure 4B). What is most noticeable in the distribution graphs are the sharp, overlapping peaks at the low EDR. For the conditions shown, over 80% of the reactor volume had an EDR under 1.5E-3 m^2/s^3 and over 95% of the reactor volume had an EDR under 1.0E-2 m^2/s^3, highlighting the uniformity in EDR throughout the reactor volume. The inset graph outlined in red within Figure 4B shows an example of the EDR distribution at a condition outside the suggested operating range (0.5 L at 60 rpm). It is evident that the peak has been significantly flattened, with larger

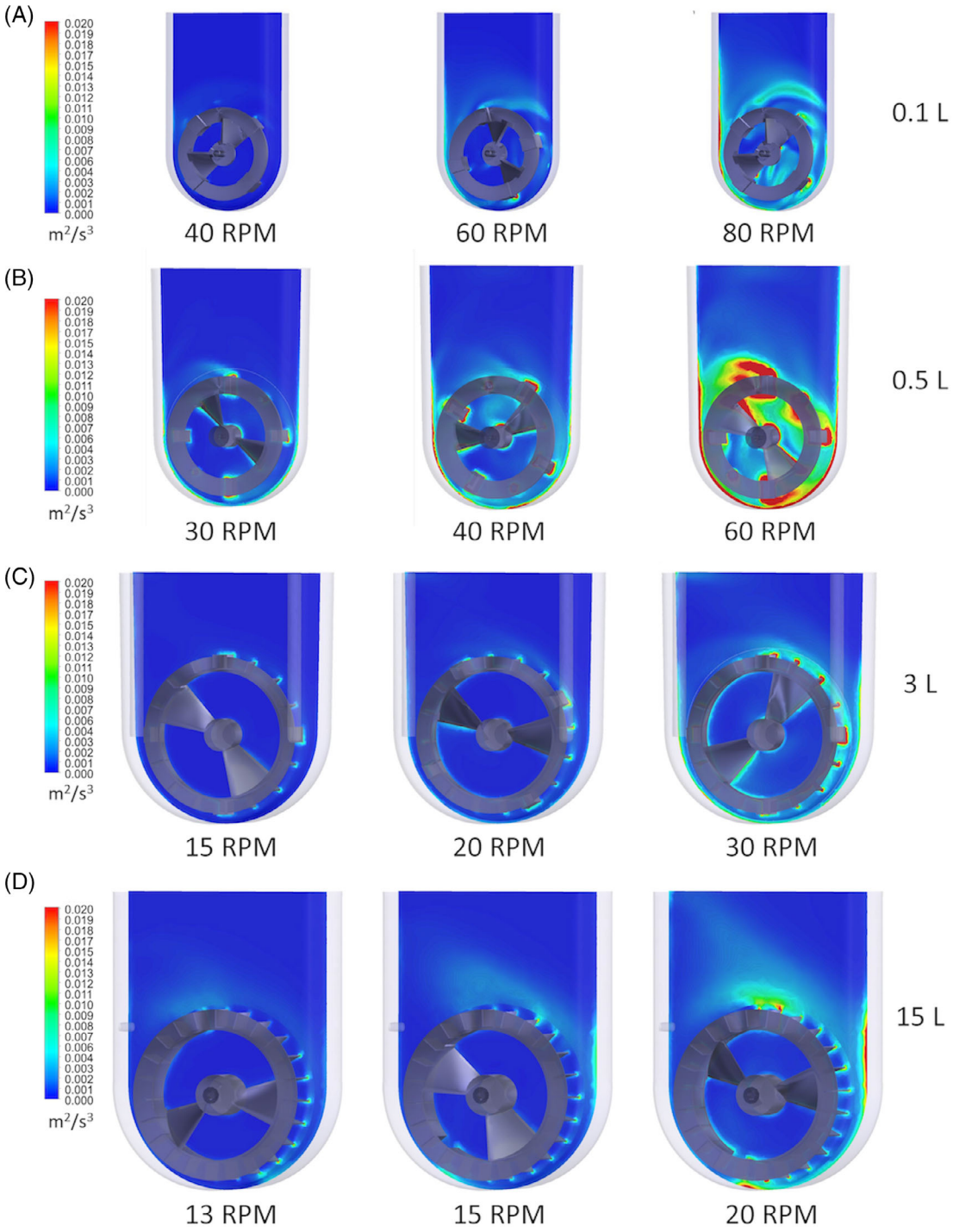

FIGURE 3 Steady-state, vertical plane heat-maps of the energy dissipation rate throughout the (A) 0.1-L, (B) 0.5-L, (C) 3-L, and (D) 15-L VW bioreactor scale. These cut planes are not imaged to scale—the following wheel diameters can be used as a reference measurement: 0.1 L (43 mm), 0.5 L (72 mm), 3 L (137 mm), and 15 L (227 mm)

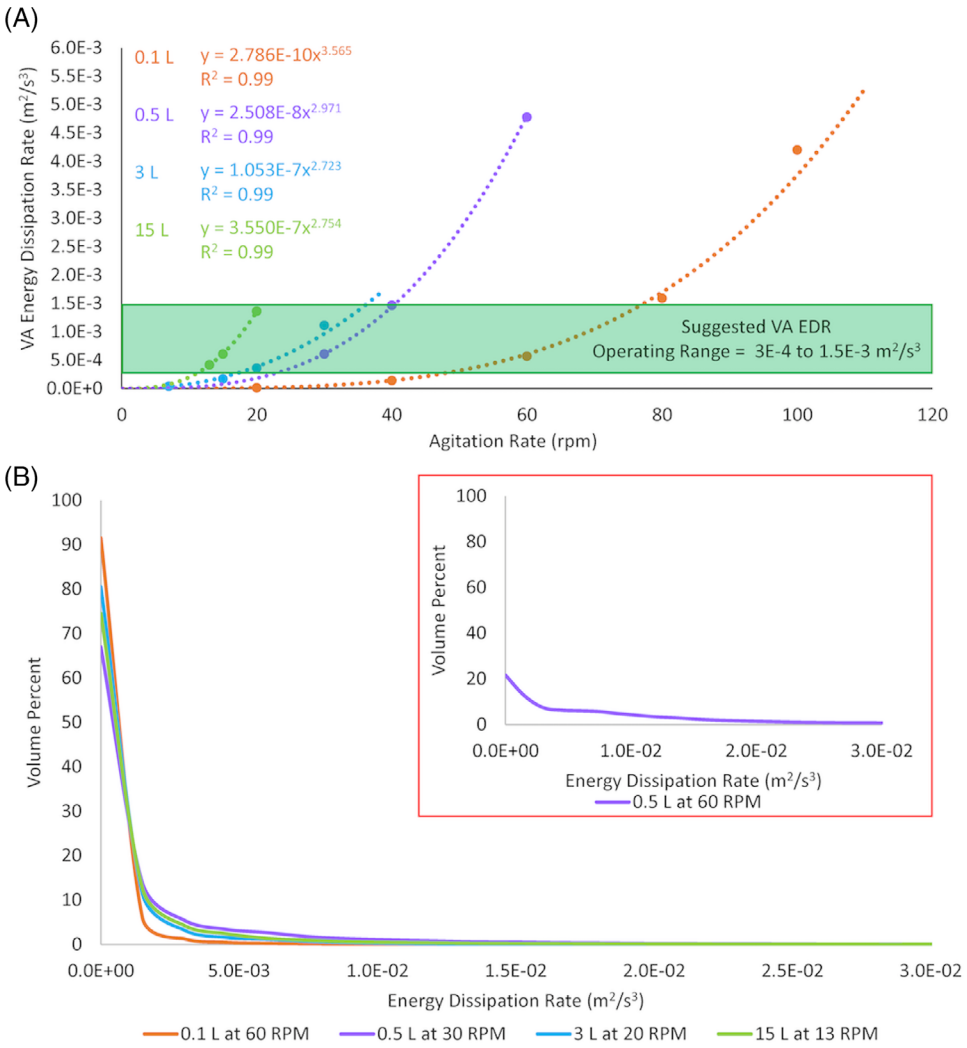

FIGURE 4 (A) Volume average energy dissipation rates (data points) versus the agitation rate of each VW bioreactor modelled. Power trendline equations (dashed lines) were generated for each bioreactor scale and a suggested operating range for hiPSC aggregate culture was defined (green box). (B) Energy dissipation rate distributions within the suggested operating range, and an example of the distribution profile outside the working range (red box)

fractions of the reactor volume at different EDRs. This provides a less optimal, more heterogenous environment for the cells.

3.3 | Culture of hiPSC aggregates in vertical-wheel bioreactors

A suggested range of VA EDRs was set for the culture of hiPSCs inoculated as single cells and cultured as aggregates in the VW bioreactors. To biologically validate the suggested working range, a variety of agitation rates at the 0.1 and 0.5 L scale were tested experimentally. A 7-day culture was run at the 0.1 L scale at 60 rpm and at the 0.5 L scale at 30 and 40 rpm, which were determined to be within the working range of VA EDRs. The 0.5 L was also run at 18 rpm, a condition outside the lower limit of the suggested operating range, and at 60 rpm, a condition outside the upper limit of the suggested operating range. Each condition was tested with two pluripotent stem cell media: STEMCELL Technology's mTeSR1 and an in-house affordable medium derived from the B8 formulation,[20] referred to as home-brew (HB) medium. Successful culture was defined by high proliferation rates, in-line with maximum fold expansions achieved in previous publications,[17,18] visually suspended aggregate culture throughout the 7-day culture period, and morphologically healthy aggregate expansion with homogeneity in aggregate sizes. Morphologically healthy aggregate expansion refers to the successful formation of aggregates on day 1 of culture, with few visible single cells remaining, as well as the growth of full, smooth, spherical aggregates that do not clump together or settle to the bottom of the bioreactor.

All tested agitation rates at the 0.1 L (60 rpm) and 0.5 L (30 and 40 rpm) scale chosen from within the suggested working range of VA EDRs were proven to provide a favourable culture environment for significant cell proliferation (Figures 5A,B). By day 7 of culture, hiPSCs cultured in mTeSR1 medium reached expansions between 27 ± 5.3 and 37 ± 1.9-fold. This is in line with optimized published reports of hiPSCs cultured in VW

bioreactors using mTeSR1 medium.[17,18] Cells cultured in HB medium reached higher expansions between 47 ± 2.9 and 62 ± 3.5-fold on day 7. Cell viabilities remained above 88% ± 1.0% and 92% ± 1.2% on day 7 when cultured in mTeSR1 and HB media, respectively. In these tested working conditions, uniform aggregate cultures formed on day 1 with almost no single cells visible in the phase contrast microscope images (Figure 5C). These

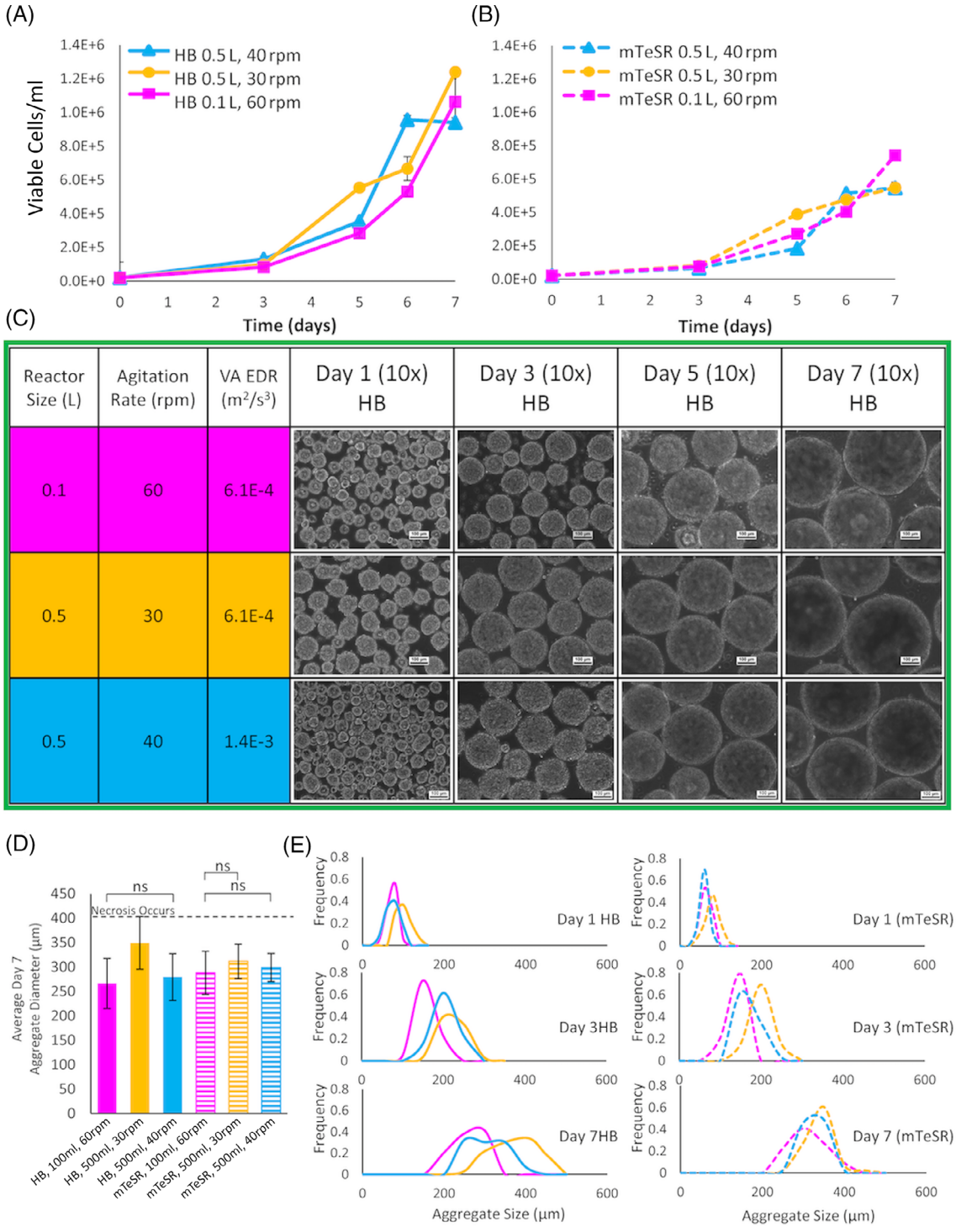

FIGURE 5 Growth curves for hiPSCs cultured in the 0.1- and 0.5-L VW bioreactors in (A) HB medium and (B) mTeSR1 medium, and (C) representative phase-contrast microscope images (10X magnification) of aggregate growth throughout the 7-day culture period in HB medium. (D) Average aggregate size on Day 7 of expansion and (E) aggregate size distributions for Days 1, 3, and 7 using HB and mTeSR1 media

aggregates continued to increase in diameter through the 7-day growth period, with notably smooth edges and homogeneity in average diameter within each culture condition. Uniformity within aggregate culture is particularly important for hiPSCs, where aggregate size not only impacts cell health and proliferation potential, but also plays a role in downstream processing and dictating potential differentiation biases.[21,22] Desired aggregate sizes for downstream applications must be achievable at the various bioreactor scales. Average aggregate sizes for the hiPSCs cultured in mTeSR1 and HB media at conditions within the desired range of VA EDR, were measured on day 7 (Figure 5D). It is evident that average aggregate sizes achieved at the 0.1 L scale could be reproduced at the 0.5 L scale when the bioreactors were operated within the suggested working range of VA EDRs. When cultured in mTeSR1, there were no statistical differences in day 7 aggregate sizes between the 0.1 L bioreactor run at 60 rpm and the 0.5 L bioreactor run at either 30 or 40 rpm, and when cultured in HB medium, there were no statistical differences in day 7 aggregate sizes between the 0.1 L bioreactor run at 60 rpm and the 0.5 L bioreactor run at 40 rpm. It should be noted that the aggregates cultured in HB medium in the 0.5 L bioreactor at 30 rpm were statistically larger on day 7. In addition, for all conditions tested within the suggested working range of VA EDR, the average aggregate diameters remained below 400 μm, where cell necrosis has been proven to result due to diffusion limitations of oxygen and nutrients.[10] Aggregate size distribution graphs for day 1, day 3, and day 7 are presented for cells cultured in HB and mTeSR1 media (Figure 5E). Throughout the culture period, aggregate size distributions overlap one another for all conditions tested with mTeSR medium within the suggested operating ranges. Aggregate size homogeneity is also evident by the narrow, single peaks with each distribution. This overlap in distributions throughout the culture period also holds true for the 0.1 L bioreactor operated at 60 rpm and the 0.5 L bioreactor operated at 40 rpm when cultured in HB medium. There is a shift in this distribution curve towards a larger average aggregate size on day 7 for the 0.5 L bioreactor cultured at 30 rpm in HB medium. This highlights the importance of continuous monitoring of aggregate size distribution patterns over time and demonstrates that the models presented in this study are not always perfect at predicting exact agitation rates for maintaining aggregate sizes when scaling up using different process variables. These limitations may be further emphasized when scaling up from the 0.1 L bioreactor, which produced a much greater deviation in the equation exponent for the VA EDR versus rpm correlation compared to the larger scale bioreactors. Working within the suggested operating range, however, has been proven here to provide a very good estimation on where to start when choosing agitation rates for biological experiments.

Average Kolmogorov length scales were calculated based on VA-EDR values, according to standard equations.[12] For the 0.1 L bioreactor at 60 rpm, 0.5 L bioreactor at 30 rpm, and 0.5 L bioreactor at 40 rpm, the average Kolmogorov length scales were 180, 178, and 142 μm, respectively. The aggregates shown in Figure 5E started off generally smaller than these values and ended up generally larger. Within this operating range, there was no trend in aggregate size versus VA-EDR or Kolmogorov length scale. It is unclear if hydrodynamic removal of cells from the surface of the aggregates was substantial. The eddy lengths are above those known to correlate with damage in microcarrier cultures.[9,23]

Conditions outside the lower (0.5 L at 18 rpm) and upper (0.5 L at 60 rpm) range of suggested working VA EDRs were tested to compare growth and aggregate morphology to a working control bioreactor operated within the range of suggested VA EDRs (0.5 L at 30 rpm). As predicted, the hydrodynamic environments outside the suggested operating range did not support healthy aggregate growth throughout the culture period, resulting in a culture failure point when operating below the lower limit and significantly decreased cell yields when operating above the upper limit (Figure 6A). In the culture operated below the lower limit, on day 1, aggregates did form; however, they were larger than those formed within the working range conditions, and not uniform in size (Figure 6B). These aggregates continued to grow as nonuniform clusters. By day 4 and day 5 for the HB and mTeSR1 medium conditions, respectively, all the cell aggregates had clumped together into large flakes too heavy to be suspended throughout the bioreactor, settling and sticking to the bottom of the vessel. In the culture operated above the upper limit, aggregates formed and continued to expand; however, proliferation and final cell yields were significantly reduced. Importantly, as predicted through our CFD simulations, the wide distribution of EDRs within the bioreactor operated above the suggested working range resulted in aggregate size heterogeneity, decreasing the overall quality of the bioreactor culture. On day 6, from 4X phase contrast microscope images shown as part of Figure 6A, it is evident that there is a large distribution in aggregate sizes at the end of the culture period when operated above the suggested working range (outlined in orange) compared to the uniform distribution in aggregate sizes that appear when operating within the suggested working range (outlined in green). The average Kolmogorov length scale for culture above the suggested range was 106 μm, well into the range that correlates with damage in microcarrier

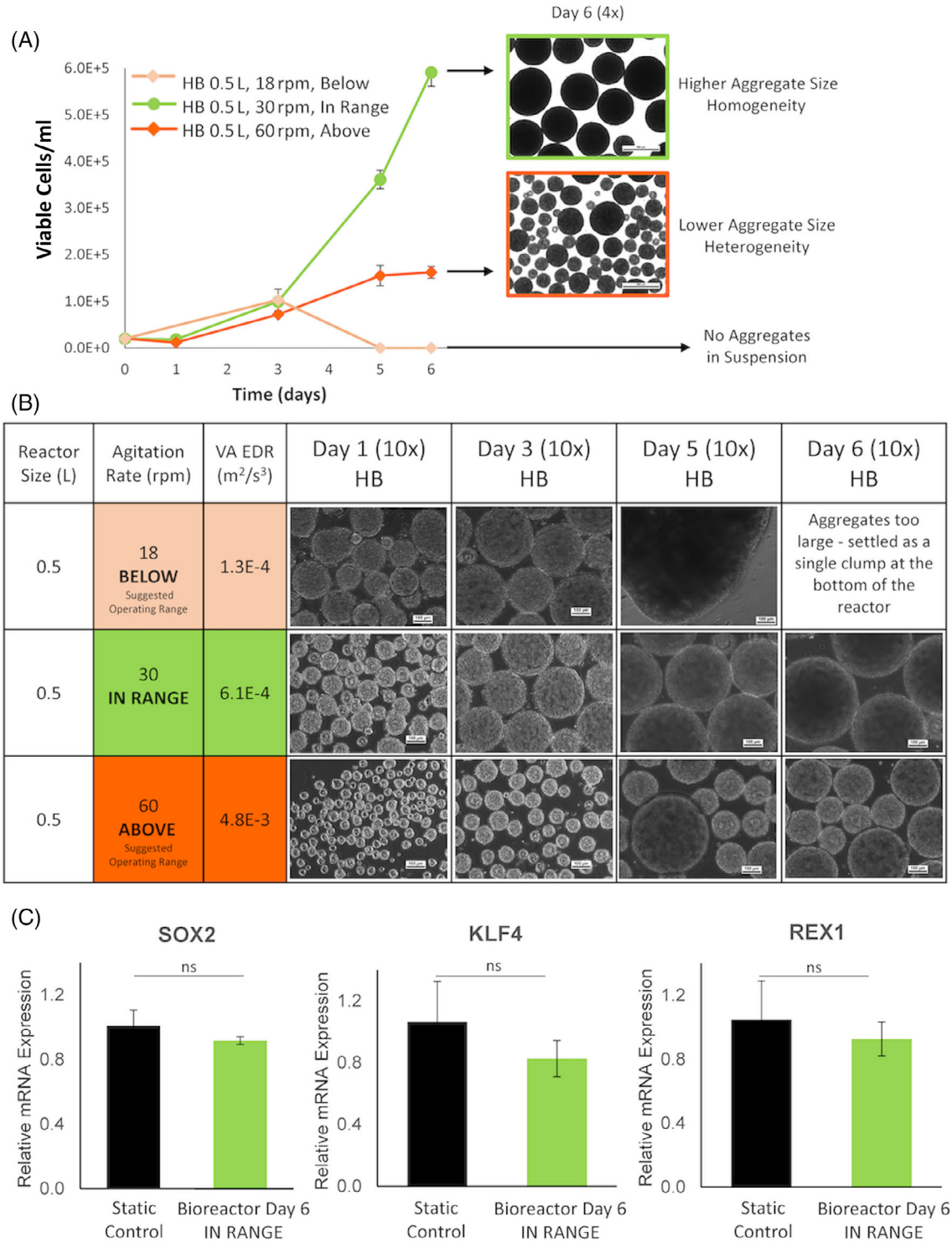

FIGURE 6 (A) Growth curves for hiPSCs cultured in the 0.5-L VW bioreactors in HB medium at agitation rates below, in range, and above the suggested operating range with (B) representative phase-contrast microscope images (10X magnification) of aggregate growth. (C) Expression levels of pluripotency-associated genes, SOX2, KLF4, and REX1. hiPSCs cultured in static conditions were used as a reference sample (Static Control) to analyze the changes in gene expression following expansion in VW bioreactors for 6 days (Bioreactor D6 Control IN RANGE). Transcript levels were normalized to an internal reference gene human GAPDH and expressed relative to the static control

cultures.[9,23] That said, there is often not a simple relationship between Kolmogorov length scale and aggregate size.[9,23]

Cells from day 6 of the working bioreactor control (0.5 L at 30 rpm in HB medium) were tested to compare relative expression of pluripotency genes SOX2, KLF4,

and REX1 with static control hiPSCs cultured on Matrigel. There were no statistically significant differences in gene expression between the bioreactor culture and static controls, indicating maintenance of pluripotency.

3.4 | Comparison of calculated versus measured volume-average energy dissipation rates

Experimental measurements of VA EDRs for VW bioreactors have recently become available.[24] A large range of data was collected for the PBS 0.5 L VW bioreactor, using water, glycerol, and water-glycerol mixtures. The resulting plot of Power number versus Reynolds number showed a clear laminar flow regime for Reynolds numbers below 50, with the expected slope near −1. Flow likely in the turbulent regime, or at least near the turbulent regime, was observed for Reynolds numbers above 2700, with the expected slope near 0. Data in the turbulent regime was also collected for the PBS 3 L and 15 L VW bioreactors, for Reynolds numbers of 8400 and above, very clearly showing the expected slope of 0. In the turbulent or near turbulent regime (Re > 2700), the resulting average Power numbers were 0.99, 0.87, and 1.11 for the PBS 0.5, 3, and 15 L, respectively. There are small differences in geometry that likely account for the small differences in Power number across scales. No measured data is yet available for the 0.1 L bioreactors, or the 0.5 L bioreactors below 28 rpm with water, due to challenges in measuring very low torque levels. As a result, there is no measured data for Reynolds numbers between 700–2700. There is a chance the transition to turbulence occurs at a Reynolds number somewhat below 2700, such as at 2000 or so.

For the turbulent or near turbulent regime (Re > 2700), Figure 7 shows the comparison of the CFD calculated VA EDRs from the current study against the measurements discussed above. With some scatter, there is good correlation between the calculated and measured values, with the calculated values sometimes higher and sometimes lower than the measured values. Some of the discrepancies can potentially be explained by differences in probe configurations between the measured and modelled set-ups. These issues will be addressed in future studies.

For turbulent flow, the expected slope of VA EDR versus agitation rate is 3.[25] All the sets of calculated and measured data in Figure 7 show slopes near this expected value. For the turbulent or near turbulent regime (Re > 2700), Figure 8 shows the comparison of Power numbers calculated via CFD (from VA-EDRs) versus ones determined from the measurements discussed above. The Power numbers are plotted against Reynolds numbers, and were both determined via standard equations.[25,26] The average power numbers calculated via CFD were 1.21, 0.61, and 0.96 for the PBS 0.5, 3, and 15 L, respectively. These differ by +22%, −30%, and −14%, respectively, versus those determined from measurement and discussed above (0.99, 0.87, and 1.11, respectively). With some scatter, there is good correlation between the calculated and measured values, with an average difference of just −7.3%. Again, some of discrepancies can potentially be explained by differences in probe configurations between the measured and modelled set-ups. Others have found some differences between Power numbers calculated via CFD and measured values including Nienow et al.[26] Further refinement of the CFD modelling and experimental techniques will hopefully reduce the differences.

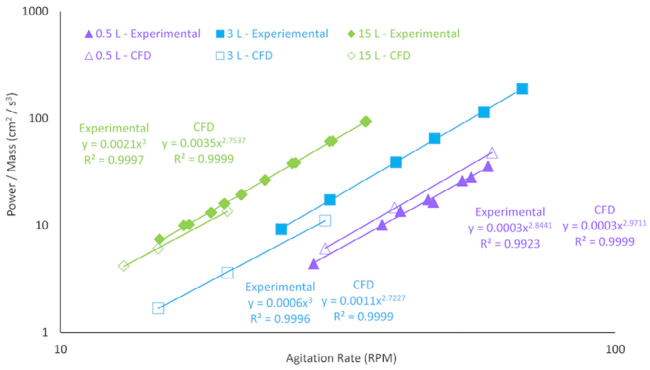

FIGURE 7 Power/mass versus agitation rate comparing experimentally derived data from Croughan et al. to CFD-predicted values for the 0.5-, 3.0-, and 15-L VW bioreactors[24]

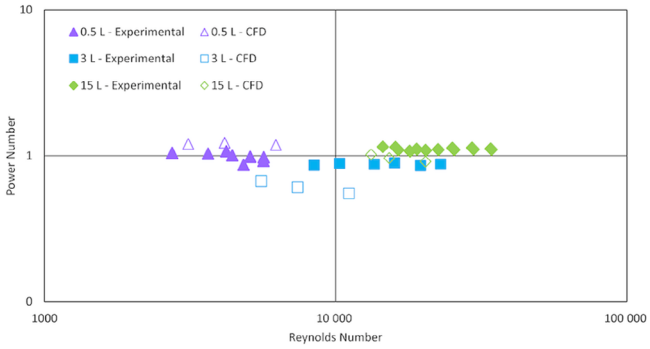

FIGURE 8 Power number versus Reynolds number comparing experimentally derived data from Croughan et al. to CFD-predicted values for the 0.5-, 3.0-, and 15-L VW bioreactors[24]

4 | DISCUSSION

Traditionally, bioreactor scale-up predictions are performed using empirical relationships based on maximum

values or average values.[12,15,19] However, these scale-up equations were developed primarily for stirred suspension bioreactors with cylindrical vessel geometries and horizontal blade or turbine impellers.[16] As such, they do not account for unique vessel and impeller geometries such as the VW bioreactor or the addition of measurement and sample probes. To overcome these challenges, the current study used CFD modelling to map out the hydrodynamic environment inside VW bioreactors of various scales. CFD modelling allows for changes in the bioreactor geometry, such as modification to the impeller geometry or the inclusion of probes which affects the resulting hydrodynamic forces, to be accounted for. Therefore, it provides a more accurate representation of the complete hydrodynamic environment. Additionally, CFD modelling can be used to calculate maximum values which in turn can predict regions of damaging forces to cells. However, these maximum values represent a small volume fraction of the vessel. Therefore, they provide a poor representation of the overall hydrodynamic environment throughout the vessel. This can lead to a lack of understanding of the cell culture environment and poor predictions for scale-up agitation rates. As an alternative, the current study used CFD modelling to determine the volume average hydrodynamic environment. Since CFD requires the modelled volume to be divided into small elements, average hydrodynamic values within the vessel geometry can be calculated, providing a broader picture of the fluid behaviour throughout the vessel rather than at a single location. Furthermore, the distribution of energy dissipation can be used for comparison of maximum local values across changes in scale and geometry. To date, studies using the volume average hydrodynamic environment have not encountered situations where maximum values were the determining factor for scale up.[16,27]

Previous studies have observed that the fluid in a laboratory scale 0.1 L VW bioreactor moves in a lemniscate pattern throughout the entire volume of the reactor.[23,28] The velocity heat maps generated in the current study demonstrate this fluid flow pattern is mimicked through the various scale VW bioreactors. This fluid pattern is a result of the unique impeller geometry with peripheral paddles and oppositely oriented axial vanes which combine radial mixing in the vertical plane and axial mixing in the horizontal plane of the vessel, creating bidirectional fluid flow. It has been previously demonstrated that with traditional horizontal-blade bioreactors, the fluid flow moves in a predominately axial direction.[13,29–31] This results in cells or cell aggregates potentially getting trapped in either high shear (around the impeller centre plane) or low shear (top and bottom dead zones) environments instead of continuously circulating through all regions and being subjected to true VA hydrodynamic forces. The lemniscate pattern of fluid in the laboratory scale 0.1 L VW bioreactor was also observed in the three modelled scales of larger VW bioreactors, providing justification that the VW bioreactor is a scalable platform.

CFD modelling also revealed that low, relatively homogeneous EDRs could be achieved in the VW bioreactors. EDR is the rate at which turbulent kinetic energy is converted to thermal internal energy through viscous shear stress. It is extensively used as an alternative to shear stress to characterize flow conditions.[32] As seen in EDR heat maps, relatively small increases in EDR occur throughout the bioreactor volume, represented by the predominately dark blue cut planes. This indicates that low EDR is maintained at all scales of the VW bioreactor and further supports the scalability of the platform. Like the lemniscate pattern, the low EDRs observed are attributed to the geometry of the vessel. The impeller is designed to occupy a large proportion of the vessel space. This increases the fluid contact area to dissipate the rotational energy generated. As a result, gentler mixing can occur compared to traditional stirred suspension bioreactors which possess a wide range of EDR values. This provides a more suitable environment for cell aggregates.

Although the VW bioreactor results in more efficient mixing due to the lemniscate pattern and lower EDRs, the use of CFD modelling allowed areas of relatively high hydrodynamic values to be identified. As demonstrated from the heat maps for both VA velocity and EDR, regions of different colours were observed at the outer edge of the impeller. These regions became more prominent as the agitation rate was increased for each scale. This observation is aligned with previous studies that have shown that the high shear and EDR areas occur around the impeller.[33,34] Although these values exist, they represent a very small fraction of the overall volume of the vessel. This supports the claim that traditional scale-up equations, based upon maximum local values, cannot be used for appropriate scale-up as they do not account for the hydrodynamic values for the bulk of the fluid. Importantly, the maximum values observed in the VW bioreactor are much lower than those in traditional stirred suspension bioreactors. Previous CFD studies with traditional stirred bioreactors have reported over a million-fold range in local EDR values.[23]

In addition to providing further insight about the hydrodynamic environment, CFD modelling was used to develop scale-up correlations that allow for the prediction of VA EDR based on changes in agitation rates. Maintaining a constant VA EDR when moving from small to large scales has proven to be more effective than maintaining a constant VA shear rate when used to

predict agitation rates for scale-up of aggregate cultures, as cell interactions with turbulent eddies strongly influence aggregate size. Aggregates in the culture that are smaller than the eddies are engulfed, and aggregates that are larger are sheared apart. As shown from the results of this study, the use of a VA EDR scale-up strategy allowed for the expansion of hiPSC aggregates of consistent size while maintaining uniform EDR distributions at various vessel volumes. This highlights the effectiveness of using CFD and VA EDR as a scale-up approach. It should also be noted that the use of CFD modelling in this study allowed for the volume average Kolmogorov eddy size to be estimated based on the VA EDR, as shown in Section 3.3, for results in the turbulent or near turbulent regime (Re > 2700). This knowledge can possibly be used to predict when detrimental effects will occur, although a further study would be needed.

The use of CFD modelling provided insights on the hydrodynamic environment within the VW bioreactor and generated data to create scale-up correlations for the different scales. However, there are limitations to these models. In the development, a k-epsilon turbulent model was used. Although this is a frequently used model to simulate the hydrodynamic environment of suspension bioreactors, one critical assumption is that the fluid motion is turbulent.[15,19] As discussed previously, turbulent or near turbulent flow has been observed for the VW bioreactors when the Reynolds number is 2700 or higher. For culture fluid at 37°C with a kinematic viscosity of 0.0071 cm^2/s,[9] this condition is achieved at 63, 23, 6.4, and 2.3 rpm for the PBS 0.1, 0.5, 3, and 15 L VW bioreactors, respectively. The low end of the recommended range of VA EDR is 3.4E-4 m^2/s^3. Based upon the CFD calculations, with the correlations shown in Figure 4A, this condition is achieved at 51, 25, 19, and 12 rpm for the PBS 0.1, 0.5, 3, and 15 L VW bioreactors, respectively. Thus, the low end of the recommended range of VA EDR is in the turbulent or near turbulent regime for the PBS 0.5 L and larger VW bioreactors. For the PBS 0.1 L, it is possibly in the higher end of the transitional flow regime. As discussed previously, additional data is needed to determine the transition point more accurately into turbulence. It may occur at a Reynolds number of 2000. If so, the low end of the recommended range for the PBS 0.1 L would be in the turbulent regime.

The suggested VA EDR working range for hiPSC aggregate culture was validated at the 0.1 and 0.5 L scale. Agitation rates inside and outside this suggested range were tested to evaluate cell proliferation, aggregate morphology, and aggregate size. The 0.1 and 0.5 L are the smallest VW bioreactors available and were chosen for biological validation to save media costs, allowing multiple conditions to be tested in parallel. Due to the similarity in geometry between all VW bioreactors, it is likely that the five-fold volume increase from the 0.1 to 0.5 L scale tested should mimic the six-fold volume increase from the 0.5 to 3 L scale and the five-fold increase from the 3 to the 15 L.

To validate the working range and robust nature of the expansion protocol, two hiPSC media types were used for each bioreactor condition. mTeSR1 is, to date, the mostly widely published feeder-free cell culture medium for hESCs and hiPSCs.[35] We have previously published optimized protocols for hiPSC aggregate culture in VW bioreactor using mTeSR1.[17,18] These protocols, which were adapted for use in this study, aimed to maximize cell fold expansion using minimal resources while maintaining high pluripotent cell quality over multiple serial passages in the bioreactor. In this study, we were able to reproduce these high proliferation rates using mTeSR1 at both the 0.1 and 0.5 L scale, reaching a maximum expansion of 37-fold in 7 days.

The HB medium used in the study was created in-house as a chemically defined, lower cost alternative to commercially available media. HB medium was adapted by altering the concentration of bFGF and adding 1% NEAA from the successful B8 formula developed for static culture of hiPSCs.[20] The HB medium alternative, which had not yet been tested in a suspension culture system, was selected as a lower cost option for affordable protocol development when moving towards large-scale production. HB medium also eliminates albumin, which is a common constituent of most academic and commercial media formulae. Elimination of human and animal protein products including human serum albumin and fetal bovine serum is ideal for both cost savings and increasing reproducibility between runs performed with different lots. It is well documented that serum additives are ill-defined and highly variable, hampering both basic and clinical research.[36]

The aggregates cultured in HB medium in the VW bioreactor appeared morphologically healthy with similar average aggregate sizes and distributions compared to the mTeSR1 conditions, and resulted in an even higher proliferation rate, reaching a maximum expansion of 62-fold in 7 days. These are amongst the highest published expansion profiles for hiPSC culture. While studies have investigated the expansion of hiPSCs in traditional horizontal-blade bioreactors, they achieve only moderate cell fold increases and require increased nutrients resources. Specifically, early publications demonstrated a maximum of 6-fold expansion in 4–7 days,[37] while recent publications reported a maximum of 10- to 13-fold expansion in 5 days,[38] and 10- to 16-fold expansion in 7 days.[39] Even more recently, a study by Manstein et al. achieved 70-fold cell expansion in 7 days.[40] However, a

greater feeding regime to increase cell yields in a perfusion mode was required, whereas the current study utilized minimal feeding in a fed batch process. The ability to consistently achieve these high fold expansions at various bioreactor scales drastically improves the potential for hiPSCs to be used in a variety of applications spanning regenerative medicine fields, disease modelling, drug discovery, and pharmacogenomics.

In addition to achieving high cell proliferation rates, it was of utmost importance to ensure the suggested working conditions could produce morphologically healthy aggregates of uniform size. It has been noted that when working with PSCs, lineage specific differentiation can be affected by the size of colonies, aggregates, and embryoid bodies,[41–43] making homogeneity in aggregate size within the bioreactor necessary for a successful culture. It was evident from the phase contrast microscope images taken throughout the cultures that healthy aggregate morphology, growth, and size distributions were achieved for all conditions tested within the suggested working range of VA EDRs. As noted in a study by Manstein et al., aggregate sizes increase throughout the culture period through cell proliferation and aggregate conglomeration—when two or more aggregates come together to form a larger aggregate. Similarly, cell death and aggregate shearing—dividing larger aggregates into smaller subsets and single cells—causes a decrease in aggregate sizes.[40] The overlap in aggregate distributions between conditions tested within the suggested operating range throughout the culture period suggest that the aggregate growth kinetics are maintained between the hydrodynamic conditions.

When aggregate size heterogeneity does occur, it is often a result of ineffective mixing in the bioreactor. It is likely that this occurs when some aggregates spend more time in high EDR zones (around the impeller), leading to smaller average diameters, and some aggregates spend more time in low EDR zones (near the top of the working volume,) leading to larger average diameters. This bimodal heterogeneity in aggregate sizes was observed as early as day 1 for the VW bioreactor condition tested below the suggested lower limit working range (0.5 L at 18 rpm) and above the suggested upper limit working range (0.5 L at 60 rpm). The authors have also previously encountered heterogeneity in aggregate size as an obstacle when culturing hiPSCs as aggregates in horizontal-blade stirred suspension bioreactors.[18] It was also important for average aggregate sizes to remain under 400 μm in diameter, where cell necrosis has proven to result due to diffusion limitations of oxygen and nutrients.[10] This size limitation impacts the potential for cell expansion. It is one reason the adapted protocol used with single-cell seeding at low inoculation densities is advantageous—as it allows for an increased culture period and fold expansion prior to aggregate harvesting.

Finally, it should be noted that a limitation to this study is the functional testing of cell pluripotency maintenance following bioreactor expansion. Previous work using the same cell line, mTeSR1 medium, and 0.1 L VW bioreactors demonstrated that hiPSCs maintained pluripotency phenotype and function following several serial passages within the bioreactor based on qPCR analysis, karyotyping, teratoma formation, and directed differentiation.[17,18] In the present study, relative expression of pluripotency genes SOX2, KLF4, and REX1 of hiPSCs cultured in HB medium in a static control vessel and a 0.5 L VW bioreactor showed no difference in expression, which was used as one positive indication of pluripotency maintenance.

5 | CONCLUSIONS

In this study, CFD modelling was used to characterize and analyze the hydrodynamic environment of VW bioreactors to be used as a scale-up platform for hiPSC aggregate culture. Each bioreactor scale (0.1, 0.5, 3, and 15 L) was modelled at a minimum of three agitation rates to allow for the generation of scale-up correlations that could be used to predict larger bioreactor operating conditions based on lower cost experiments conducted at the small scale. A suitable operating range of VA EDRs was defined for the successful culture of hiPSC aggregates inoculated as single cells. This suggested operating range defines agitation values within each VW bioreactor scale that would result in high cell expansion rates, and healthy aggregate formation, growth, and uniformity. This operating range was biologically validated at the 0.1 and 0.5 L scale with two PSC culture media used for each bioreactor condition tested. It was shown that the VW bioreactors provide an optimal environment for hiPSC culture that can be mimicked throughout scale-up.

ACKNOWLEDGEMENTS

We thank Pete Dry and Dan Thompson for their assistance in developing and simplifying the SolidWorks models used for this study. We also thank the University of Calgary for allowing us use of the Advanced Research Cluster and Dr. Dmitri Rozmanov and Dr. Ian Percel for their guidance in developing our scripts. Additionally, we thank Yas Hashimura for his guidance in selecting the agitation rates for each scale. TD was funded by a NSERC USRA. BB was partially funded by a Vanier Canada

Graduate Scholarship. We also thank the University of Calgary URGC for funding.

CONFLICT OF INTEREST

Breanna Borys, Hannah Worden, Abigail Blatchford, and Sunghoon Jung are employees of PBS Biotech, Inc. Matt Croughan is a Scientific Advisory Board member and consultant for PBS Biotech, Inc. Brian Lee is CEO and co-founder of PBS Biotech, Inc. These collaborating authors participated in the development of the bioreactors used in the manuscript as well as the experimental concept design and data review. PBS Biotech, Inc. provided financial support for the researchers to complete the study. This does not alter the authors' adherence to all the policies of the journal. All other authors declare no competing interests.

PEER REVIEW

The peer review history for this article is available at https://publons.com/publon/10.1002/cjce.24253.

REFERENCES

[1] S. Sart, Y. J. Schneider, Y. Li, S. N. Agathos, *Cytotechnology* **2014**, *66*, 709.
[2] C. A. Rodrigues, D. E. Nogueira, J. M. Cabral, *Cell and Gene Therapy Insights* **2018**, *4*, 791.
[3] Y. Shi, H. Inoue, J. C. Wu, S. Yamanaka, *Nat. Rev. Drug Discov.* **2017**, *16*, 115.
[4] M. Serra, C. Brito, C. Correia, P. M. Alves, *Trends Biotechnol.* **2012**, *30*, 350.
[5] S. Stolberg, K. E. McCloskey, *Biotechnol. Progr.* **2009**, *25*, 10.
[6] M. A. Kinney, C. Y. Sargent, T. C. McDevitt, *Tissue Eng. Part B-Re.* **2011**, *17*, 249.
[7] T. Gareau, G. G. Lara, R. D. Shepherd, R. Krawetz, D. E. Rancourt, K. D. Rinker, M. S. Kallos, *J. Tissue Eng. Regen. M.* **2014**, *8*, 268.
[8] S. C. Nath, B. Day, L. Harper, J. Yee, C. Yu-Ming Hsu, L. Larijani, L. Rohani, N. Duan, M. S. Kallos, D. E. Rancourt, *Stem Cells* **2021**, https://doi.org/10.1002/stem.3382.
[9] M. S. Croughan, E. S. Sayre, D. I. C. Wang, *Biotechnol. Bioeng.* **1989**, *33*, 862.
[10] A. P. Van Winkle, I. D. Gates, M. S. Kallos, *Cells Tissues Organs* **2012**, *196*, 34.
[11] G. Catapano, P. Czermak, R. Eibl, D. Eibl, R. Pörtner, in *Cell and Tissue Reaction Engineering* (Eds: R. Eibl, D. Eibl, R. Pörtner, G. Catapano, P. Czermak), Springer, Berlin, Germany **2009**, p. 173.
[12] A. W. Nienow, *Cytotechnology* **2006**, *50*, 9.
[13] B. S. Borys, E. L. Roberts, A. Le, M. S. Kallos, *Biochem. Eng. J.* **2018**, *133*, 157.
[14] S. Abbasalizadeh, M. R. Larijani, A. Samadian, H. Baharvand, *Tissue Eng. Part C-Me.* **2012**, *18*, 831.
[15] W. J. Kelly, *Biotechnol. Appl. Bioc.* **2008**, *49*, 225.
[16] M. Shafa, K. M. Panchalingam, T. Walsh, T. Richardson, B. A. Baghbaderani, *Biotechnol. Bioeng.* **2019**, *116*, 3228.
[17] B. S. Borys, T. So, J. Colter, T. Dang, E. L. Roberts, T. Revay, L. Larijani, R. Krawetz, I. Lewis, B. Argiropoulos, D. E. Rancourt, S. Jung, Y. Hashimura, B. Lee, M. S. Kallos, *Stem Cell. Transl. Med.* **2020**, *9*, 1036.
[18] B. S. Borys, T. Dang, T. So, L. Rohani, T. Revay, T. Walsh, M. Thompson, B. Argiropoulos, D. E. Rancourt, S. Jung, Y. Hashimura, B. Lee, M. S. Kallos, *Stem Cell Res. Ther.* **2021**, *12*, 55.
[19] S. Kaiser, C. Loffelholz, S. Werner, D. Eibl, in *Computational Fluid Dynamics: Technologies and Applications* (Ed: O. Minin), InTech, London, UK **2011** Ch. 4.
[20] H. H. Kuo, X. Gao, J. M. DeKeyser, K. A. Fetterman, E. A. Pinheiro, C. J. Weddle, H. Fonoudi, M. V. Orman, M. Romero-Tejeda, M. Jouni, M. Blancard, T. Magdy, C. L. Epting, A. L. George, P. W. Burridge, *Stem Cell Rep.* **2020**, *14*, 256.
[21] C. Kropp, D. Massai, R. Zweigerdt, *Process Biochem.* **2017**, *59*, 244.
[22] B. Abecasis, T. Aguiar, E. Arnault, R. Costa, P. Gomes-Alves, A. Aspegren, M. Serra, P. M. Alves, *J. Biotechnol.* **2017**, *246*, 81.
[23] M. S. Croughan, D. Giroux, D. Fang, B. Lee, in *Stem Cell Manufacturing* (Eds: J. M. S. Cabral, C. L. da Silva, L. G. Chase, M. M. Diogo), Elsevier, Amsterdam, The Netherlands **2016** Ch. 5.
[24] S. Croughan, D. Giroux, S. Guerra, N. Starkweather, Y. Hashimura, B. Lee, S. Jung, unpublished.
[25] P. M. Doran, *Bioprocess Engineering Principles*, 2nd ed., Elsevier, Amsterdam, The Netherlands **2013** Ch. 8.
[26] A. W. Nienow, C. D. Rielly, K. Brosnan, N. Bargh, K. Lee, K. Coopman, C. J. Hewitt, *Biochem. Eng. J.* **2013**, *76*, 25.
[27] B. S. Borys, A. Le, E. L. Roberts, T. Dang, L. Rohani, C. Y.-M. Hsu, A. A. Wyma, D. E. Rancourt, I. D. Gates, M. S. Kallos, *J. Biotechnol.* **2019**, *304*, 16.
[28] J. C. Kim, J. H. Seong, B. Lee, Y. Hashimura, D. Groux, D. J. Oh, *Biotechnol. Bioproc. E.* **2013**, *18*, 801.
[29] P. Sucosky, D. F. Osorio, J. B. Brown, G. P. Neitzel, *Biotechnol. Bioeng.* **2004**, *85*, 34.
[30] H. Singh, S. H. Teoh, H. T. Low, D. W. Hutmacher, *J. Biotechnol.* **2005**, *119*, 181.
[31] K. A. Williams, S. Saini, T. M. Wick, *Biotechnol. Progr.* **2002**, *18*, 951.
[32] M. Mollet, N. Ma, Y. Zhao, R. Brodkey, R. Taticek, J. J. Chalmers, *Biotechnol. Progr.* **2004**, *20*, 1437.
[33] R. S. Cherry, K. Kwon, *Biotechnol. Bioeng.* **1990**, *36*, 563.
[34] H. D. Laufhütte, A. Mersmann, *Chem. Eng. Technol.* **1987**, *10*, 56.
[35] mTeSR™1, https://www.stemcell.com/mtesr1-standardized-medium-for-the-feeder-independent-maintenance-of-hescs-hipscs.html (accessed: June 2021).
[36] M. Wu, Z. B. Han, J. F. Liu, Y. W. Wang, J. Z. Zhang, C. T. Li, P. L. Xin, Z. C. Han, X. P. Zhu, *Cell. Physiol. Biochem.* **2014**, *33*, 569.
[37] R. Zweigerdt, R. Olmer, H. Singh, A. Haverich, U. Martin, *Nat. Protoc.* **2011**, *6*, 689.
[38] G. Meng, S. Liu, A. Poon, D. E. Rancourt, *Stem Cells Dev.* **2017**, *26*, 1804.
[39] C. K. Kwok, Y. Ueda, A. Kadari, K. Günther, S. Ergün, A. Heron, A. C. Schnitzler, M. Rook, F. Edenhofer, *J. Tissue Eng. Regen. M.* **2018**, *12*, e1076.

[40] F. Manstein, K. Ullmann, C. Kropp, C. Halloin, W. Triebert, A. Franke, C. M. Farr, A. Sahabian, A. Haase, Y. Breitkreuz, M. Peitz, O. Brüstle, S. Kalies, U. Martin, R. Olmer, R. Zweigerdt, *Stem Cell Transl. Med.* **2021**, *10*, 1063. https://doi.org/10.1002/sctm.20-0453.

[41] C. L. Bauwens, R. Peerani, S. Niebruegge, K. A. Woodhouse, E. Kumacheva, M. Husain, P. W. Zandstra, *Stem Cells* **2008**, *26*, 2300.

[42] Y. S. Hwang, G. C. Bong, D. Ortmann, N. Hattori, H. C. Moeller, A. Khademhosseinia, *P. Natl. Acad. Sci. USA* **2009**, *106*, 16978.

[43] A. W. Xie, B. Y. K. Binder, A. S. Khalil, S. K. Schmitt, H. J. Johnson, N. A. Zacharias, W. L. Murphy, *Sci. Rep.* **2017**, *7*, 14070.

SUPPORTING INFORMATION

Additional supporting information may be found online in the Supporting Information section at the end of this article.

How to cite this article: T. Dang, B. S. Borys, S. Kanwar, J. Colter, H. Worden, A. Blatchford, M. S. Croughan, T. Hossan, D. E. Rancourt, B. Lee, M. S. Kallos, S. Jung, *Can. J. Chem. Eng.* **2021**, 1. https://doi.org/10.1002/cjce.24253